Turkish Journal of Engineering
https://dergipark.org.tr/en/pub/tuje
e-ISSN 2587-1366

Optimization of the convergent-divergent nozzle tip and reducing the acoustic energy

Kumaran Thirugnanasambantham [1*], Balaji Elangovan[2], Swetha SreeRangaiah[1], Raja Kannan[3], Sarangapani Palani[4], Murugu Nachippan Nachiappan[4]

[1]Department of Aeronautical engineering, Acharya Institute of technology, Bengaluru*
[2]Department of Mechanical Engineering, SRM institute of Science and Technology, Ramapuram, Chennai
[3] Vel Tech Rangarajan Dr.Sagunthala R&D Institute of Science and Technology, Chennai
[4]Department of Automobile Engineering, Easwari engineering college, Chennai

Cite this study: Kumaran T et.al., (2025). Optimization of the convergent-divergent nozzle tip and reducing the acoustic energy, Turkish Journal of Engineering, 9 (3), 417-424.

https://doi.org/10.31127/tuje.1561759

Keywords
Delaval nozzle
CFD
Modified Nozzle Tip
Aeroacoustics

Research Article

Received:05.10.2024
Revised:19.11.2024
Accepted:29.11.2024
Published:01.07.2025

Abstract

One of the practical components that can be found in aircraft engines, the Delaval nozzle, works to improve the aircraft's performance in terms of its stability and its capacity to manoeuvre at different speeds of operation. This research concentrates on the acoustic behaviors shown by this nozzle during the transition from low rate to sonic speed. The modification of the nozzle tip at various degrees of inclination on the transition velocity is the procedure used to minimize the amount of acoustic energy emitted. The acoustic behavior is analyzed based on the FW-H acoustics model utilized, and the optimization problem is solved using the practical eddy simulation approach in CFD. The acoustic Power, measured in dB, is estimated at various angles on the nozzle tip, and the performance of the Delaval nozzle is used to show how the redesigned nozzle tip affects the nozzle's acoustic behavior.

1. Introduction

Modern technology is becoming more prevalent; therefore, the worldwide commercial aviation fuel nozzle 2016-2020 report was created with assistance from industry professionals. Aircraft engines are large, complex machinery subjected to a great deal of stress. Engine pipe or tube that control conditions and rate flow speed, direction, mass shape, pressure, and reaction forces enter the enclosed chamber as a mainstay and high performance of aircraft; it also wants the fuel-efficient and decreases noise. Emissions, engine pipes, or tubes that control conditions and rate flow speed, direction, mass shape, pressure, and reaction forces enter the enclosed chamber as a mainstay of an aircraft's high performance. Also, it wants the fuel-efficient. It decreases noise, and emissions, engine pipe or tube that control limits condition and rate flow speed, Using the first rule of thermodynamics in the engine. The nozzle's operation is described because it generates higher thrust and is mostly dependent on geometry. Turbojets and turboprops are two different types of nozzles. Based on geometry, the convergent nozzle or convergent-divergent nozzle is what we call it (CD). The central nozzles are where the main flow departs. The annular nozzle is where the fan flow exits. We aim to develop the nozzle tip and increase the nozzle's and aircraft's performance. It reduces noise and significantly reduces noise from all individual sources that contribute to the increased noise. Consequently, increasing the number of chevrons reduces the nozzle's Acoustic Power Level. In this project, the lowest Acoustic Power Level compared to other nozzles, indicating that this form of chevron nozzle aids in noise reduction. As a result, the chevron nozzle's static pressure reaches the same ideal level as the baseline round nozzle. The outcome of the Acoustic

power level study reveals that it has a lower value at the exit than the baseline nozzle [1]. The nozzle and key components of an aviation engine are discussed in this article. The piston created a lot of noise and engine noise, and it has a lot of temperature and speed variations. Using Solid Works, this research looked at chevron nozzle analysis, design parameters, and design [2]. This work focuses on designing an inlet and outlet with various configurations, including normal, convergent, and venture kinds. CFD has been used to examine the air flow through each developed manifold. In order to achieve effective combustion, an optimised intake manifold that enables the most airflow within the cylinder was chosen after comparing the analysis results. [3-4].

The innovative 2D exhaust nozzle for minimizing IR signature is demonstrated here, and the design process for meeting thermal and structural criteria utilizing thermo-structural analysis. For the first time, the 2D exhaust nozzle is employed. for dispersing high-temperature core gas flows and increasing mixing performance with bypass air flows as a sequence of composite layers with elliptical cross-sections [5]. The engine application test confirmed that the extreme temperature of the Proposed exhaust nozzle was kept below 100 ◦ C, and the IR signature was also reduced by 20% compared to the Coaxial exhaust nozzle. Changing the thickness of the C-SiC layer, insulator layer, ad CFRP layer constituting the 2D exhaust nozzle, nozzle abrasion resistance, structural strength, and heat transfer to the outermost nozzle surface can be controlled [6]. According to the data, the notched nozzle lowered broadband jet noise compared to the baseline nozzle, and the level of noise reduction was comparable to a serrated nozzle. Notched Nozzles, Turbofan Engine for Noise Tests, and Data Acquisition are validated experimentally using CFD. Then they explained more about nozzle tip creation and jet noise reduction [7]. The nozzle was compressed to a sufficient length using a nonlinear compression approach. Then, with the goals of thrust and lift force, a Surrogate-based optimization of three design variables, namely the pressure ratio of the nozzle's exhaust to ambient, the Initial expansion ratio, and the average compression ratio, was done, yielding a Pareto optimum front [8-10]. The vast majority of CFD simulations of aerospace applications use Reynolds-averaged Navier–Stokes (RANS) closures to account for the effects of turbulence. There are also diagrams of the nozzle in four distinct configurations. The circle denotes the measurement, whereas the bar denotes the variation in the measurement bar over many realizations of the experiment. Such matching boundaries may be seen on the turbulent kinetic energy profiles [11-12].

The lift ratio difference between airfoils with various nozzles decreases under subsonic and two-dimensional conditions. When the pitch angle of the airfoil is set at 8 degrees, the lift of the airfoil decreases as the conformal nozzle height rises. With the rate of change, the jets travel at the double the mainstream speed [13-14]. Finally, such ideas are straightforward to implement and have the potential to significantly reduce noise in the exhaust nozzle of an aircraft engine. When these redesigned nozzles are used, the noise level of the exhaust stream is lowered by around 20%. Low-speed secondary flow & chevron variations give superior acoustic sound pressure compared to a simple type [15-16].

1.1 Noise reduction

Over the years, several researchers have worked on ways to reduce the noise of aero nozzles, including the alteration of the nozzle's exit and the boundary layer's interaction with the nozzle's interior walls via partial notches. According to research, vortices formed by the gaps cut at the nozzle exit help reduce jet noise [21] one portion of a wave. Turbulence on a big scale is utilized to represent jet noise generation. In this method, an analogous source is determined regarding the two-space-time relation of fluid pressure on a circular surface around the jet plume. This correlation is used to analyze the force applied by the jet plume. The surface is close enough to the turbulent flow zone to be influenced by non-propagating fluid dynamic fingerprints of extensive turbulent features. Still, it is also far enough away from the turbulent flow region that linear behavior may be assumed when transferring the relatively close pressure to the sound domain—measurement of pressure statistics right beyond the jet boundary layers to capture traces of large-scale turbulence. Microphones are arranged so that they are close enough to the turbulent flow region to pick up the hydrodynamic pressure there but far enough away so that nonlinear source terms may be ignored [22].

Measurement, analysis, and quantification of the acoustic pressure near a speaker. To accomplish this goal, a brand-new post-processing method centered on the wavelet's implementation is given. As the technique separates acoustic stress and hydrodynamic pressure, the roughly Gaussian background variations are perceived as background noise [23] the use of wavelets in aeroacoustics, focusing on compressible jet data analysis in particular. Conditional statistics, acoustical and fluid dynamics pressure physical separation, and stochastic modeling are the three wavelet-based process control approaches examined in this paper. Experimental data from a turbulent jet's near field is used as a test case for three different approaches [24]. The NASA GRC BASS code, a quadratic constructed CAA solution, would be evaluated on a CAA standard problem. Using a conventional grid generator and a fully curved grid, this test attempts to determine the impact of the higher response methods employed in CAA on a practical approach to the flow path and unstable waves [25].

2. Method

The method of optimizing the nozzle in the divergent portion is modified with variable angles dimensional parameters like length of the nozzle, inlet and exhaust diameter, several chevrons (modified tip), and length chevron for the design of baseline. Then various tip angles are considered for the modelling of the nozzle. In each case, the tip angle is increased by a 10-degree angle.

The solution and boundary conditions are applied to the CFD. The solution model for acoustics and turbulent model is initiated in the commercial software for the analysis. The governing equation for a nozzle considered is derived using inviscid, irrotational, and isentropic characteristics. The following equations were obtained from [12] to get the asymmetric flow and plane flow for the nozzle in equation 2.

$$\{\{(u^2 - a^2)u_x + (v^2 \_ a^2)v_x + 2uvu_y - \delta a^2 v/y = 0, u_y - v_x = 0 \quad \text{..... (1)}$$

$$\{(\frac{dy}{dx}) = \Lambda\pm = tan\ tan(\theta \pm \alpha)$$

$$(u^2 - a^2)du_{\pm} + (2uv - (u^2 - a^2)\Lambda \pm)dv_{\pm} - \left(\frac{\delta a^2 v}{y}\right) dx_{\pm} = 0 \quad \text{..... (2)}$$

Where δ =n and δ = 0 indicate the flow which we consider for the evaluation, and θ and α are the flow angle and Mach angle, then u and v are the x and y direction velocities. The following equations calculated other parameters in the finite difference method based on characteristic lines, which calculate the pressure, specific heat, velocity, and temperature.

A polynomial characterizing the thermophysical parameters of the gas is included with varying specific heat in the above equation [13].

$$Ma_4 = \frac{V_4}{\sqrt{\gamma RT_{tin}}} - \frac{\gamma^{-1}}{2} V_4^2, \text{.....(3)}$$

$$P_{tin} = \left(1 + \frac{\gamma^{-1}}{2} Ma_4^2\right) 1^{\frac{\gamma}{\gamma-1}} P_4 \text{.....(4)}$$

$$T_{tin} = \left(1 + \frac{\gamma^{-1}}{2} Ma_4^2\right) T_4 \text{.....(5)}$$

After that while solving the computation fluid dynamic problem in these types of nozzles we have to use

$$C_p = a_1 + a_2 T + a_3 T^2 + a_4 T^3 + a_5 T^4 \text{.....(6)}$$

$$\text{Integral of } CpdT = H_4 = \frac{1}{2} V_4^2 \text{.....(7)}$$

$$P_4 = P_{tin} e^{-\frac{1}{R}\ integral\ with\ respect\ to\ time\ of\ \frac{1}{T} CpdT} \text{.....(8)}$$

A polynomial characterizing the thermophysical parameters of the gas is included with varying specific heat in the above equation [13].

2.1. Antisymmetric exit nozzle

A variety of aerial aircraft utilizes Spanwise oblique exit nozzles due to their stealth, aerodynamic, and acoustic benefits. The scream characteristics and details of the screech source structure are demonstrated by jets in the shape of rectangles that exhibit spanwise oscillations. These nozzles were successful in showing transversely antisymmetric modes of scream and spanwise antisymmetric or symmetric forms of scream. It was feasible to construct an immense range of kinematically permissible modes of motion by superimposing two non-uniform nozzles on top of one another [26]. Because of the connectivity, the twin jet in the "V" configuration has a larger contact area than the arrowhead arrangement does. Even though an additional spanwise oblique mode was seen in the single jet configurations, the twin jet station exhibited antisymmetric and symmetric coupling. It was discovered that the pressures in the inter-nozzle regions were 7.5 dB greater in the case of symmetrical coupling than in the case of anti-symmetrical coupling [27]. Large-eddy simulations are utilized to investigate the acoustic fields of a supersonic free jet under transitional conditions. The Mach number is 2.1, and the Reynolds number is 70,000. A computer model is utilized to investigate transitional supersonic jets with variable shear layer thicknesses and those with a fixed shear layer thickness [28 - 32].

2.2. Fast Fourier transform

The frequency analysis utilizes a rapid Fourier transform with a discrete Fourier transform (FFT). Simple goniometric functions, such as sines and cosines, can be constructed from any periodic signal or function using the Fourier series. The Fourier approach is well known for decomposing a complex function into a series of simple functions. Modal parameters of vibrating systems can be determined using this method. Digital wave files can be used to record the noise generated by a vibrating system and then process it further. An efficient approach for discrete Fourier transformation, the Fast Fourier Transform (FFT) reduces computation time from N2 to Nlog2N, where Na is the number of discrete signal samples [33-40].

3. Modelling and Finite element analysis

The modified nozzle tip based on the baseline angle of 40 deg,50 deg, and 60 deg configuration of the Delaval nozzle is designed in catiaV5 for the simulation purpose in CFD. The model is shown in Figure 1. Then the geometrical constraints were initialized and updated in simulation to update the meshing to solve in the solver. The mesh generated in the convergent-divergent nozzle is generated by tetra four on the model used for the simulation shown in Figure 2.

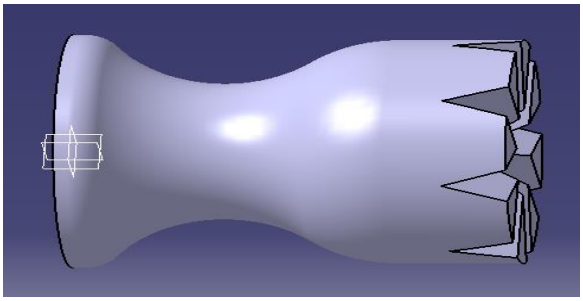

Figure 1. Modelling of the variable tip nozzle

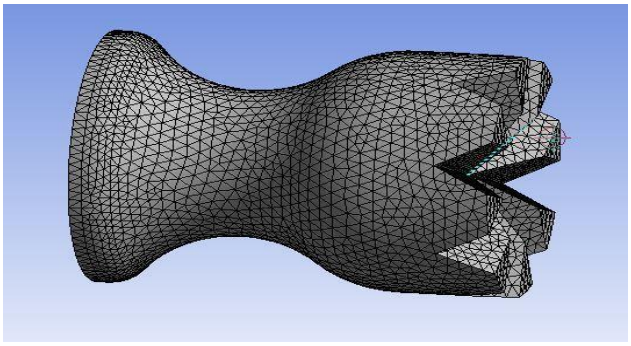

Figure 2. Meshing of the variable tip nozzle

The mesh is done in commercial software ANSYS mechanical meshing and setting the element size 0.005mm to generate finite element node for adapt the solution to solve the acoustic equation for better iterative condition suitable for least square method.

4. Results and discussions

In order to solve the obtained meshed model, the boundary conditions and model constraints needed to be taken into consideration. The solution was started with a pressure-based solution on the turbulent model for the solution that had a subsonic inlet velocity of 264 meters per second, and the pressure was normalized with gauge pressure. The solution consisted of two different situations, with the first one beginning with an evaluation of the properties using a k-epsilon model.

4.1. Pressure contour on the asymmetric nozzle

Figure 3 depicts the pressure contour that results from using a convergent-divergent model that was developed with a baseline angle of forty degrees. It demonstrates that the pressure is rising at the beginning but falling as it approaches the outlet. Therefore, the diameter of the nozzle is increasing as a result of this data.

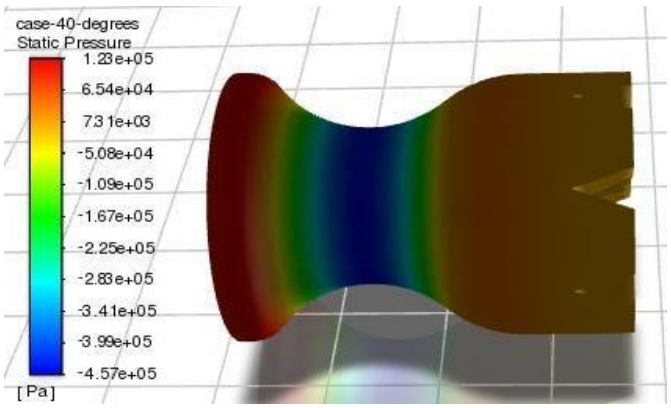

Figure 3. Pressure at 40 Degree Base angles

When compared to the air flow, the pressure on the wall of the convergent diverging nozzle is more susceptible to being influenced by acoustic energy, and the average value derived from the numerical calculations is approximately 7310 N/m^2 at the exit.

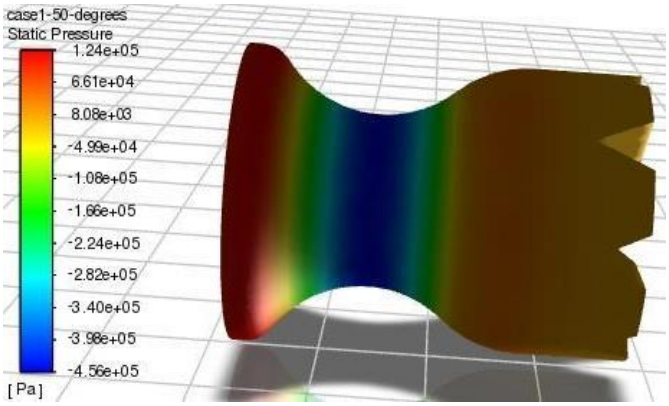

Figure 4. Pressure at 50 Degree Base angle

Comparatively, the pressure at the outlet is higher in Figure 4 when compared to the design with a base angle of 40 degrees. Which shows that variable considered to simulate the convergent divergent nozzle, from the contour it is evidently shows that a small modification on the geometry can create a change in properties especially in the fig pressure is about 8080 N/m^2, which shows that a small change on the geometry can create a change in properties. In comparison to previous designs, the pressure generated by the model with the modified base angle of 50 degrees is higher.

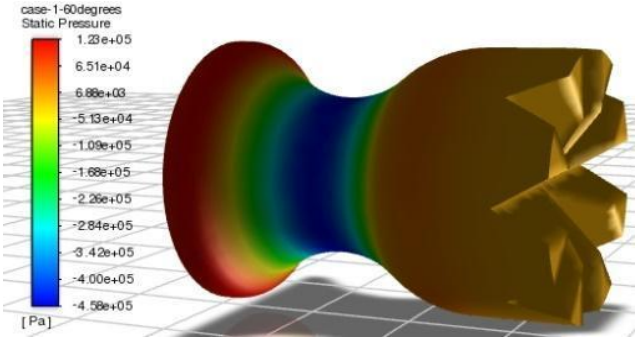

Figure 5. Pressure at 60 Degree Base angle

When compared to previous designs, the chevron divert angle on the nozzle shown in Figure 5 has a larger angle, and the nozzle also has a greater capacity for expansion when it exits. This is shown in the variation of the nozzle exit that is shown in Figure 5. In the part where the divergence is occurring, the pressure is going down. This indicates that there is the potential for the amount of acoustic energy to be decreased. After the neck, the pressure is approximately 6880N/m^2, as seen in Figure 5. In comparison to the other design scenarios, this pressure is extremely low.

4.2. Acoustic power contour on the asymmetric nozzle

After the boundary conditions for the solution in FLUENT have been established, we start the acoustics problem, and then the solution is thought of as one acoustic model, activating the FW-H acoustics model to solve with acoustic broadband noise considerations in order to evolve the acoustic power that is generated in the output boundaries and wall boundaries of the C-D nozzle that is shown in Figure 6.

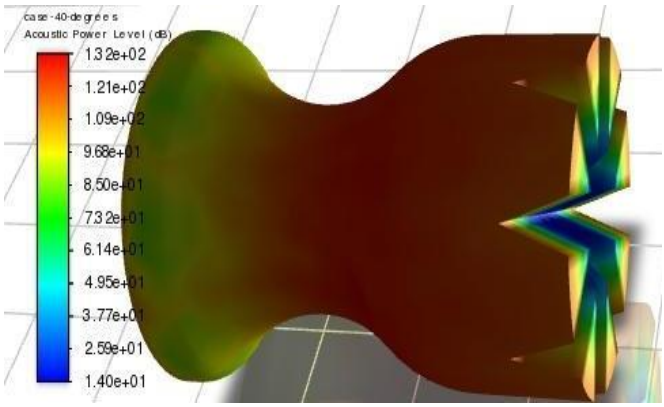

Figure 6. Acoustic Power at 40 Degree Base angle

According to the data presented in figure 6, the acoustic power level dB is rather high in the wall borders; however, this value fluctuates with respect to the variable geometry optimization, and the value of the acoustic level at exit falls somewhere in the range of around 121 dB. Therefore, in contrast to the pressure exit shown in Figure 3, the level of sound pressure that is produced by the nozzle as it exits the base angle of 40 degrees is quite high

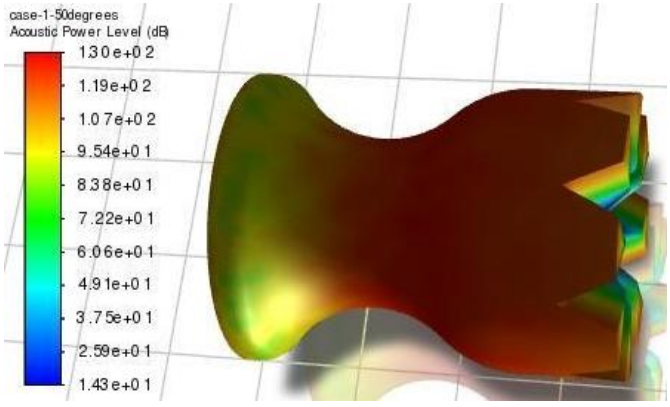

Figure 7. Acoustic Power at 50 Degree Base angles

Then, for case 2, using the same boundary conditions and velocity, we solved the acoustic model for the meshed nozzle. The exit pressure level is high in figure 4, and the acoustic power level in figure 7 indicates that the sound power level is in the range of 107 dB. Therefore, based on this, we evidently see that the acoustic power dB is decreasing by utilizing this 50-degree base angle optimization.

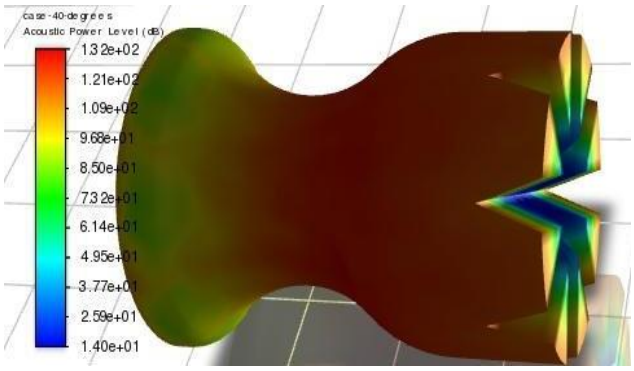

Figure 8. Acoustic Power at 60 Degree Base angle

Therefore, the acoustic power level of this model starts with 107 dB to 132 dB when considering the initial case for a 40-degree, 50-degree, or 60-degree base angle design. The remaining case, which considers for the evaluation shown in Figures 6, 7, and 8, explains how the variation of the acoustic Power based on the design is calculated. According to the results and estimates presented in figure 8, the nozzle exit of the modified design with a base angle of sixty degrees has an acoustic power level of 109 decibels.

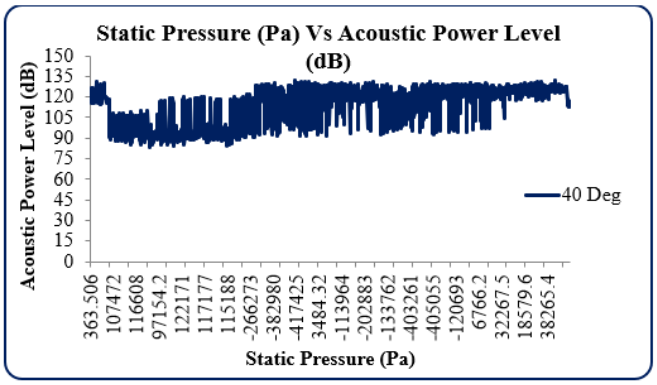

Figure 9. Static pressure Vs. Acoustic Power for 40 Degree baseline angle configuration

After working out the solution, the calculated results of the static pressure and the acoustic power generated on the wall of the convergent-divergent nozzle have been presented in Figure 9 for a baseline design with a 40-degree angle. It demonstrates the acoustic power level in relation to the static pressure that is ultimately generated after the throat has a dB level of 126 correspondingly. When we examine the data from pressure and acoustic contour in the design with a 40-degree baseline angle, the acoustic power level is somewhere in the range of 121dB to 126dB. This data is based on the pressure level at the exit.

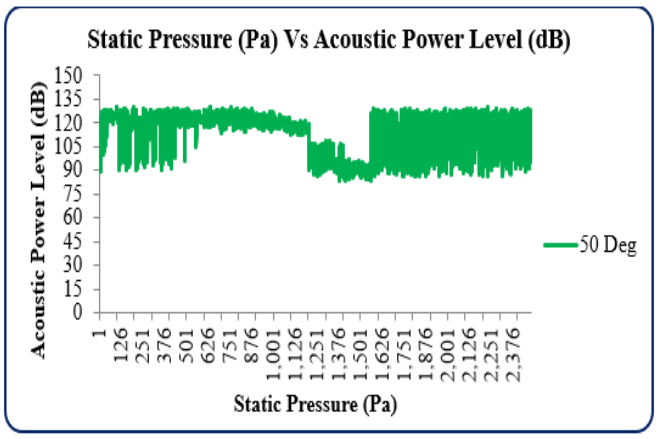

Figure 10. Static pressure Vs. Acoustic Power for 50 Degree baseline angle configuration

In a similar fashion, the results of the static pressure and the acoustic power generated on the wall of the convergent-divergent nozzle are plotted in figure 10. This figure demonstrates that the pressure level of the exit to the wall and the acoustic power level is somewhere in the range of approximately 107dB to 119dB for the case of a base angle of 50 degrees. It is clear from the evaluation that the pressure that is maintained on the wall condition and the departure of the nozzle also have an effect on the acoustic energy.

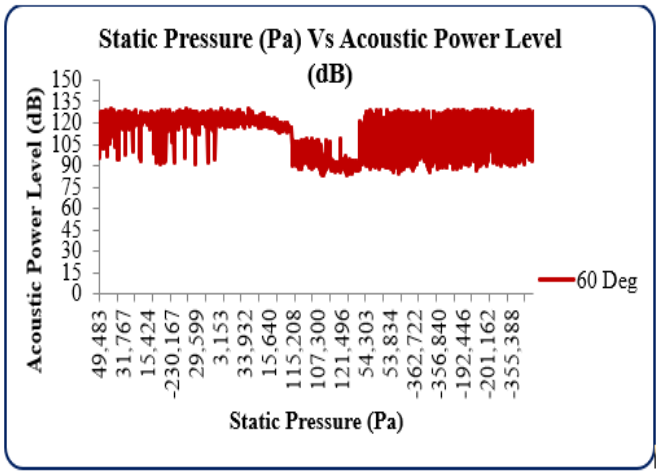

Figure 11. Static pressures Vs. Acoustic Power for 60 Degree baseline angle configuration

Based on these evaluations of the CFD analysis in three different cases, an optimized nozzle with a baseline of 60 degrees also has the same effect; however, the pressure at the exit of this type of nozzle is very low, whereas the acoustic power level at the exit of the nozzle, as shown in Figure 11, is in the range of approximately 121 dB. Almost exactly this design can also adjust to the conditions of the output nozzle. When compared across all three scenarios, the findings from the evaluation approach reveal that each possible optimization at the nozzle's exit results in a distinct degree of acoustic power.

5. Conclusion

As part of this work, a convergent diverging nozzle design was improved by adopting a range of modified and serrated nozzles developed from earlier efforts. These nozzles were derived from earlier research. Comparisons and analyses of the outcomes of this endeavour were carried out. In order to validate the pressure and acoustic characteristics of the FW-H acoustics model, a standard convergent-divergent nozzle was put through its paces in three separate test configurations. An investigation of the analysis provided the basis for determining the outcomes of this verification. On the basis of these facts, we are able to draw the conclusion that the optimization of the geometry in high-speed jet nozzles resulted in varying levels of acoustic power. However, we are going to have to select the nozzle that provides the best possible optimization in the sense that we are going to offer the 50-degree bassline optimal arrangement. Because the pressure level is manageable in comparison to the previous example that we handled, and the acoustic power level is in the range of around 107 dB to 119 dB in this scenario. According to the findings of the research that we conducted for the purpose of conducting an acoustic energy analysis in the convergent-divergent nozzle that is utilised in aircraft engines, we came to the conclusion that variable geometry nozzles prove to be effective in lowering acoustic energy levels.

Author contributions

Kumaran Thirugnanasambantham: Conceptualization, Methodology, Software. **Balaji Elangovan:** Data curation. **Swetha SreeRangaiah:** Writing-Original draft preparation, Software, Validation. **Raja Kannan**: Visualization**. Sarangapani Palani**: Investigation. **Murugu Nachippan Nachiappan:** Writing-Reviewing and Editing.

Conflicts of interest

The authors declare no conflicts of interest.

References

1. Parmar, P., Trivedi, D., Randhesiya, K., & Shingala, R. (2021). Modeling and analysis of different chevron nozzle for noise reduction. International Journal of Engineering Research & Technology (IJERT), 10(1), January 2021.
2. Akbarali, I. M., & Periyasamy, S. (2020). Design and analysis of nozzle for reducing noise pollution. IOSR Journal of Mechanical and Civil Engineering, 17, 6–12.
3. Selvam, M. A. J., Sambandam, P., & Sujeesh, K. J. (2021). Investigation of performance and emission characteristics of single-cylinder DI diesel engine with plastic pyrolysis oil and diethyl ether blends. International Journal of Ambient Energy.
4. Raja, K., & Selvam, M. A. J. (2019). Experimental investigation of four-stroke single-cylinder SI engine by modified intake manifold using computational

fluid dynamics. International Journal of Ambient Energy.
5. Zhu, M., Wang, L., Wei, F., & Du, Y. (2018). Design and optimization of the three-dimensional supersonic asymmetric truncated nozzle. Proceedings of the Institution of Mechanical Engineers, Part G: Journal of Aerospace Engineering, 232(15), 2923–2935.
6. Kim, S. J., Moon, K., Jung, H., & Choi, J. (2020). 2D exhaust nozzle with multiple composite layers for IR signature suppression. Results in Physics, 19, 103395.
7. Ishii, T., Yamamoto, K., Tanaka, H., & Suzuki, S. (2019). Jet noise reduction of turbofan engine by notched nozzle. INTER-NOISE and NOISE-CON Congress and Conference Proceedings, 259(4), Institute of Noise Control Engineering.
8. Vadla, P., & Sreekanth, S. (2018). Turbojet engine nozzle design optimization to reduce noise. IOP Conference Series: Materials Science and Engineering, 455(1).
9. Mishra, A. A., & Iaccarino, G. (2017). Uncertainty estimation for Reynolds-averaged Navier–Stokes predictions of high-speed aircraft nozzle jets. AIAA Journal, 55(11), 3999–4004.
10. Li, L., Jiang, Z., Chen, X., & Wu, T. (2017). Numerical experiment of tip-jet ducted fans with various nozzles. 53rd AIAA/SAE/ASEE Joint Propulsion Conference.
11. Clarke, J. (1976). Gas Dynamics, Volumes 1 and 2. Wiley; 772 pp. Journal of Fluid Mechanics, 87(4), 789–792.
12. Turkyilmazoglu, M. (2015). Parabolic partial differential equations with nonlocal initial and boundary values. International Journal of Computational Methods, 12(5), 1550024.
13. Kodavanla, B., Shiva, U., & Goud, M. R. (2017). Aircraft noise reduction and control system by the k–epsilon turbulence model.
14. Yang, H., Lin, Z., Zhao, M., & Chen, J. (2021). Cavitation suppression in the nozzle-flapper valves of the aircraft hydraulic system using triangular nozzle exits. Aerospace Science and Technology, 112, 106598.
15. Filippone, A. (2014). Aircraft noise prediction. Progress in Aerospace Sciences, 68, 27–63.
16. Leylekian, L., Lebrun, M., & Lempereur, P. (2014). An overview of aircraft noise reduction technologies. Aerospace Lab, 6, p-1.
17. Thomas, R. H., Lee, E., & Kumar, A. (2017). Aircraft noise reduction technology roadmap toward achieving the NASA 2035 goal. 23rd AIAA/CEAS Aeroacoustics Conference.
18. Filippone, A. (2017). Options for aircraft noise reduction on arrival and landing. Aerospace Science and Technology, 60, 31–38.
19. Kirubadurai, B., Kanagaraja, K., & Jegadeeswari, G. (2021). Analysis of knocking characteristic in dual-fuel engine—the effects on diethyl ether. INCAS Bulletin, 13(2), 83–90.
20. Sumendran, J., Shekar, K. R. C., Jegadeeswari, G., & Kirubadurai, B. (2020). Design of annular combustion chamber with different types of swirl to perform pressure drop. International Journal of Scientific and Technology Research, 9(2), 1972–1975.
21. Vishnu, J., & Rathakrishnan, E. (2004). Acoustic characteristics of supersonic jets from grooved nozzles. Journal of Propulsion and Power, 20, 520–526.
22. Reba, R., Narayanan, S., & Colonius, T. (2013). Wave-packet models for large-scale mixing noise. International Journal of Aeroacoustics, 9(4–5), 533.
23. Grizzi, S., & Camussi, R. (2011). Experimental investigation of the near-field noise generated by a compressible round jet. Journal of Physics: Conference Series, 318, 092003.
24. Camussi, R., & Meloni, S. (2021). On the application of wavelet transform in jet aeroacoustics. Fluids, 6, 299.
25. Hixon, R., Wu, J., Nallasamy, R., Sawyer, S., & Dyson, R. (2004). Comparison of numerical schemes for a realistic computational aeroacoustics benchmark problem. International Journal of Aeroacoustics, 3.
26. Raman, G. (1999). Coupling of twin supersonic jets of complex geometry. Journal of Aircraft, 36, 743–749.
27. Raman, G., Panickar, P., & Chelliah, K. (2012). Aeroacoustics of twin supersonic jets: A review. International Journal of Aeroacoustics, 11(7–8), 957–984.
28. Nonomura, T., Ozawa, Y., & Abe, Y. (2021). Computational study on aeroacoustic fields of a transitional supersonic jet. Journal of the Acoustical Society of America, 149, 4484.
29. Harčarik, T., Bocko, J., & Maslákóvá, K. (2012). Frequency analysis of acoustic signal using the fast Fourier transformation in MATLAB. Procedia Engineering, 48, 199–204.
30. Das, S. K., & Saha, A. (2024). Phase velocity of love waves as function of heterogeneity and void parameter. Turkish Journal of Engineering, 8(4), 603-610.
31. Bakır, H. (2024). Optimal power flow analysis with circulatory system-based optimization algorithm. Turkish Journal of Engineering, 8(1), 92-106.
32. Abdulkerim, S. (2024). Investigating best algorithms for structural topology optimization. Turkish Journal of Engineering, 8(1), 116-126.
33. Juraev, D. A., Shokri, A., Agarwal, P., Elsayed, E. E., & Nurhidayat, I. (2023). Approximate solutions of the Helmholtz equation on the plane. Engineering Applications, 2(3), 291–303.
34. Juraev, D. A., Agarwal, P., Elsayed, E. E., & Targyn, N. (2024). Helmholtz equations and their applications in solving physical problems. Advanced Engineering Science, 4, 54–64.
35. Juraev, D. A. . (2023). Fundamental solution for the Helmholtz equation . Engineering Applications, 2(2), 164–175.
36. Harizaj, M., & Bisha, I. (2023). A proposed power control solution for industrial application in decentralized energy production. Engineering Applications, 2(1), 16-25
37. Karaca E.O., Tanyildizi,M. & Bozkurt,N. (2022). Investigation of seismic base isolation systems and their properties. Engineering Applications, 1(1), 63-71.

38. Çimen, Ö., & Keskin, S.N.(2024). Investigation of the effect of Isparta pumice on theunconfined compressive strength and swelling pressure of clay. Advanced Engineering Science, 4, 113-119.
39. Yalçın, C., & Belgin, Ö. (2023). A multivariate statistical assessment of Vein-type U-Th enrichment in Arıklı İgnimbrites. Advanced Engineering Science, 3, 55-61
40. Yuksek, G., Muratoglu, Y., & Alkaya, A.(2022). Modelling of supercapacitor by using parameter estimation method for energy storage system.Advanced Engineering Science, 2, 67-73